TECHNICAL NOTE

D-1334

WIND-TUNNEL TESTS OF A SERIES OF 18-FOOT-DIAMETER

PARACHUTES WITH EXTENDABLE FLAPS

By Berl Gamse and Paul F. Yaggy

Ames Research Center
Moffett Field, Calif.

NATIONAL AERONAUTICS AND SPACE ADMINISTRATION

WASHINGTON   August 1962

NATIONAL AERONAUTICS AND SPACE ADMINISTRATION

TECHNICAL NOTE D-1334

WIND-TUNNEL TESTS OF A SERIES OF 18-FOOT-DIAMETER

PARACHUTES WITH EXTENDABLE FLAPS

By Berl Gamse and Paul F. Yaggy

SUMMARY

The performance, stability, and control characteristics of a series of parachutes with extendable flaps are presented for a range of free-stream velocities from 20 to 60 feet per second. The tests included the variation of both flap length and flap width. The maximum lift-drag ratio which could be obtained depended upon flap configuration, flap extension, and suspension line length. Aerodynamic data obtained during the tests indicate that the parachutes were statically stable at all values of lift-drag ratio up through the maximum value. Visual observations indicated an increase in dynamic stability as lift-drag ratio increased.

INTRODUCTION

Conventional parachutes have been used for the recovery of space vehicles, but they provided no control of the glide path and, consequently, no choice of landing site. One means of providing glide-path control is through use of an extendable flap in one side of the canopy. Tests of several flapped parachute configurations were made in the Ames 40- by 80-Foot Wind Tunnel to determine: (1) their capability to alter the glide path from that of a conventional parachute, (2) the effect of flap extension on the chute axial-force coefficient, (3) the static-stability characteristics, and (4) the response of the chute to changes in control-flap extension.

NOTATION

C_A axial-force coefficient, $\dfrac{\text{axial force}}{qS_0}$

C_D drag coefficient, $\dfrac{\text{drag}}{qS_0}$

C_L lift coefficient, $\dfrac{\text{lift}}{qS_0}$

C_m pitching-moment coefficient, $\dfrac{\text{pitching moment}}{qS_0 D_0}$

C_n yawing-moment coefficient, $\dfrac{\text{yawing moment}}{qS_oD_o}$

D_i diameter of inflated parachute, ft

D_o parachute nominal diameter, uninflated, ft

F flap length, fraction of D_o

h suspension-line length, ft

$\dfrac{L}{D}$ lift-drag ratio

q dynamic pressure, lb/ft^2

R fixed riser length, ft

S_o parachute area, uninflated, $\dfrac{\pi D_o^2}{4}$, ft^2

V free-stream velocity, fps

W flap width, number of gores

Δl flap riser extension, ft

α angle of attack, the angle between the parachute axis of symmetry and the free stream, deg (see fig. 4)

γ glide angle, arc tan $\dfrac{D}{L}$, deg

ψ angle of yaw, deg

MODEL AND APPARATUS

Model

The basic parachute used for these tests was a "Glidesail" designed and fabricated by the Radioplane Company. It had an uninflated diameter of 18 feet with a geometric porosity of 1.7 percent and a mechanical porosity of 3 percent for a total porosity of 4.7 percent. The parameters used to define the various configurations tested were the flap length in decimal fraction of the uninflated diameter, D_o, the flap width in number of gores, and the length of the suspension lines in feet. A sketch of the parachute is shown in figure 1. A listing of the configurations tested is given in table I.

Control Mechanism

Flap extension and retraction was accomplished by changing the length of the flap riser. Roll control was accomplished by differentially changing the length of the two suspension lines immediately adjacent to the flap. The mechanism for performing these functions is shown in figure 2.

Force Measurement

The forces and moments produced by the parachute were measured by two strain-gage balances, a six-component balance at the parachute attachment points, and a two-component balance mounted on a sting downstream from the parachute. The two-component balance was made so that it could pass through a 5-inch-diameter metal ring installed in the canopy vent. The purpose of this arrangement was to provide a means whereby the parachute could be displaced from trim conditions to obtain stability information. An oscillograph was used to record time histories of the forces and flap position.

The general arrangement of the model in the tunnel is shown in figures 3 and 4. The pitch plane and yaw plane were the horizontal and vertical planes, respectively.

TESTING PROCEDURE

Investigation of Lift-Drag Ratio

The variation of lift-drag ratio with flap extension was investigated by allowing the parachute to assume equilibrium positions in the pitching (horizontal) plane for various flap extensions. For configurations with 13-foot suspension lines, the sting and main strut were positioned so that the sting contributed no restraint to the canopy in the pitching plane but supported the canopy so as to eliminate any yawing due to the canopy weight. All flap configurations with 13-foot suspension lines were tested at $V = 30$ feet per second, and several configurations were tested at additional tunnel velocities of 20, 40, and 60 feet per second. The $0.15D_O$-11 configuration with 26-foot suspension lines was tested without the sting at $V = 20$ feet per second only.

Static Stability in Pitch and Yaw

The investigation of static stability in pitch and yaw was confined to the $0.2D_O$-7 configuration at flap extensions of $\Delta l/D_O = 0$, 0.056, and

0.097, and $V = 20$, 30, and 60 feet per second. The results are believed to be typical of all the configurations tested. At each condition the parachute was allowed to assume an equilibrium position. It was then forced from the equilibrium position by the sting in either the pitching or yawing plane in both positive and negative directions. The angle of attack was defined by the relative positions of the two strain-gage balances as shown in figure 4.

Control Response

Tests were made to determine the relative rate of change of lift-drag ratio with flap deflection which constitutes control response. The $0.2D_O\text{-}7$ configuration was restrained in pitch and yaw by the sting at its zero-flap extension, equilibrium angle of attack at $V = 30$ feet per second. The flap was extended to $\Delta l/D_O = 0.22$ and then retracted at constant rates. The control movement and the forces on the parachute were recorded as a function of time on the oscillograph.

ACCURACY OF DATA

The various force and moment measurements were accurate within the following limits. These values include errors involved in reading and reducing the data as well as the inaccuracy of the measuring device itself.

Lift	±1.7 percent
Drag	±0.5 percent
Pitching and yawing moments	±0.7 percent
Angle of attack	±0.5°
Flap extension	±0.012 ft

Displacements of data points from the mean curves in excess of these stated values are probably due to random load variations resulting from oscillations of the nonrigid model.

The yawing-moment coefficients were corrected for the moment produced by the weight of the canopy resting on the sting.

RESULTS AND DISCUSSION

Evaluation of Testing Technique

An evaluation of the effects of the sting on the parachute was made by testing the same configuration with and without the sting in place. Such evaluation was deemed necessary since the parachute was partially restrained in yaw, even at the pitch-trim conditions, to support the weight of the canopy. A comparison of the test results obtained with and without the sting is shown in figure 5. The agreement shown indicates the sting had little or no effect on the values of lift-drag ratio developed for a given flap deflection.

A
6
3
3

Lift-Drag Ratio

The variations of lift-drag ratio with flap extension for each of the parachute configurations with 13-foot suspension lines are shown in figure 6. The discontinuities in the curves at small flap extensions were caused by collapsing the leading-edge sails in the first skirt band. As the flap extension was increased, the leading-edge sails in the second skirt band collapsed. In general, the stall of the second skirt band determined the flap extension where the maximum lift-drag ratio was obtained. The progression of a typical leading-edge collapse is shown in figure 7.

The maximum lift-drag ratio obtained with the 13-foot suspension lines was 0.54 for the $0.10D_O$-11 parachute at a free-stream velocity of 20 feet per second. This corresponds to a glide angle, relative to the horizontal, of 61.6^O. An indication of the effect of suspension line length on lift-drag ratio is shown in figure 8 which compares results obtained for the $0.15D_O$-11 parachute with two different suspension line lengths at a free-stream velocity of 20 feet per second. It is seen that increasing the suspension line length from 13 feet to 26 feet (the fixed riser length was held constant) increased the maximum lift-drag ratio from 0.49 to 0.65 and decreased the maximum glide angle from 63.9^O to 57° relative to the horizontal. The effect of further lengthening the suspension lines is not known.

The variations with flap configuration of the maximum lift-drag ratio are shown in figure 9. These results indicate that the maximum lift-drag ratio was obtained with a configuration of $0.10D_O$ flap length and 11-gores flap width. Since the parachute is a nonrigid device, deformations due to horizontal translation could alter the axial force produced and, hence, the rate of vertical descent. However, the variation of axial force with flap extension shown in figure 10 indicates there was little change.

Stability

All of the configurations tested were statically stable in pitch and yaw. The pitching- and yawing-moment coefficients are shown in figures 11 and 12, respectively, as functions of the change in angle of attack or angle of yaw for the $0.2D_O$-7 configuration, its stability characteristics being considered typical. The lack of symmetry in the pitching-moment variations is due to a lack of longitudinal symmetry in the canopy caused by the slots at the ends of the flap. Also shown, in figure 13, are plots of C_D, α and C_m as functions of C_L for free-stream velocities of 20, 30, and 60 feet per second and for three flap extensions.

Although the parachutes were statically stable, at certain conditions (particularly at $\Delta l/D_O = 0$) they were dynamically unstable, as shown in the film supplement to this report. This film is available for loan upon request. With the flap closed, there were large angular oscillations in pitch and yaw as well as unsteady breathing.[1] As the flap was extended, increasing the porosity, the oscillations of the chute became smaller and breathing was reduced. Intermittent collapse of the leading-edge sails caused some dynamic instability, but this condition appeared to be more highly damped than when the flap was closed. As the leading-edge sails became fully collapsed, this instability diminished. These conditions are shown for the $0.2D_O$-7 configuration in the film supplement.

Control Response

A typical time history of lift-drag ratio and flap extension is shown in figure 14. The results show no time lag between the actuation of the control and the build-up of the lift force. The difference in the rates of flap extension and retraction (extension: 1.06 fps; retraction: 0.54 fps) was due to the overloading of the actuator by the drag load on the flap. It is interesting to note that when the parachute was not in equilibrium (fig. 14), the maximum value of L/D was much larger than for the equilibrium case (fig. 6).

QUALITATIVE OBSERVATIONS

Perhaps the most important result of these tests is that the maximum lift-drag ratio that could be obtained was limited to about 0.7 by leading-edge sail collapse. Making the leading edge rigid might remove this limitation. It is of interest to note that this sail collapse caused no large oscillations or instabilities of the canopy and equilibrium conditions were reestablished quickly. Increasing the length of

[1]The porosity of the test parachutes was less than that generally accepted to be required for parachutes of this size operating at the test descent velocities.

the suspension lines delayed the leading-edge sail collapse to higher values of lift-drag ratio by changing the angle of the leading-edge sail to the relative wind. However, visual observations indicated that the dynamic stability was much less for the parachute with the longer suspension lines than with the shorter lines throughout the range of lift-drag ratios studied. Further lengthening of the lines would probably produce some gains, but would be undesirable from other considerations, such as deployment, weight, and stowage.

A
6
3
3

Ames Research Center
    National Aeronautics and Space Administration
        Moffett Field, Calif., May 4, 1962.

TABLE I.- LIST OF PARACHUTE CONFIGURATIONS TESTED

Configuration	Flap length (F), fraction of D_O	Flap width (W), number of gores
$0.33D_O$-7	0.33	7
$.20D_O$-7	.20	7
$.20D_O$-11	.20	11
$.20D_O$-13	.20	13
$.15D_O$-7	.15	7
$.15D_O$-9	.15	9
[1]$.15D_O$-11	.15	11
$.15D_O$-13	.15	13
$.11D_O$-7	.11	7
$.10D_O$-11	.10	11

[1]Both 26-foot suspension lines and 13-foot suspension lines tested.

A
6
3
3

Vent ring

9"

F   W

D_O

D_i

h

Suspension line

R

Flap riser

Fixed riser

Steering line

TOTAL NUMBER OF GORES = 28

W = Flap width, no. of gores
F = Flap length, fraction of
       D_O
D_O = Uninflated diameter, 18'
D_i = Inflated diameter, $\sim$12'
h = Suspension line length,
       13' or 26'
R = Fixed riser length, 1.5'
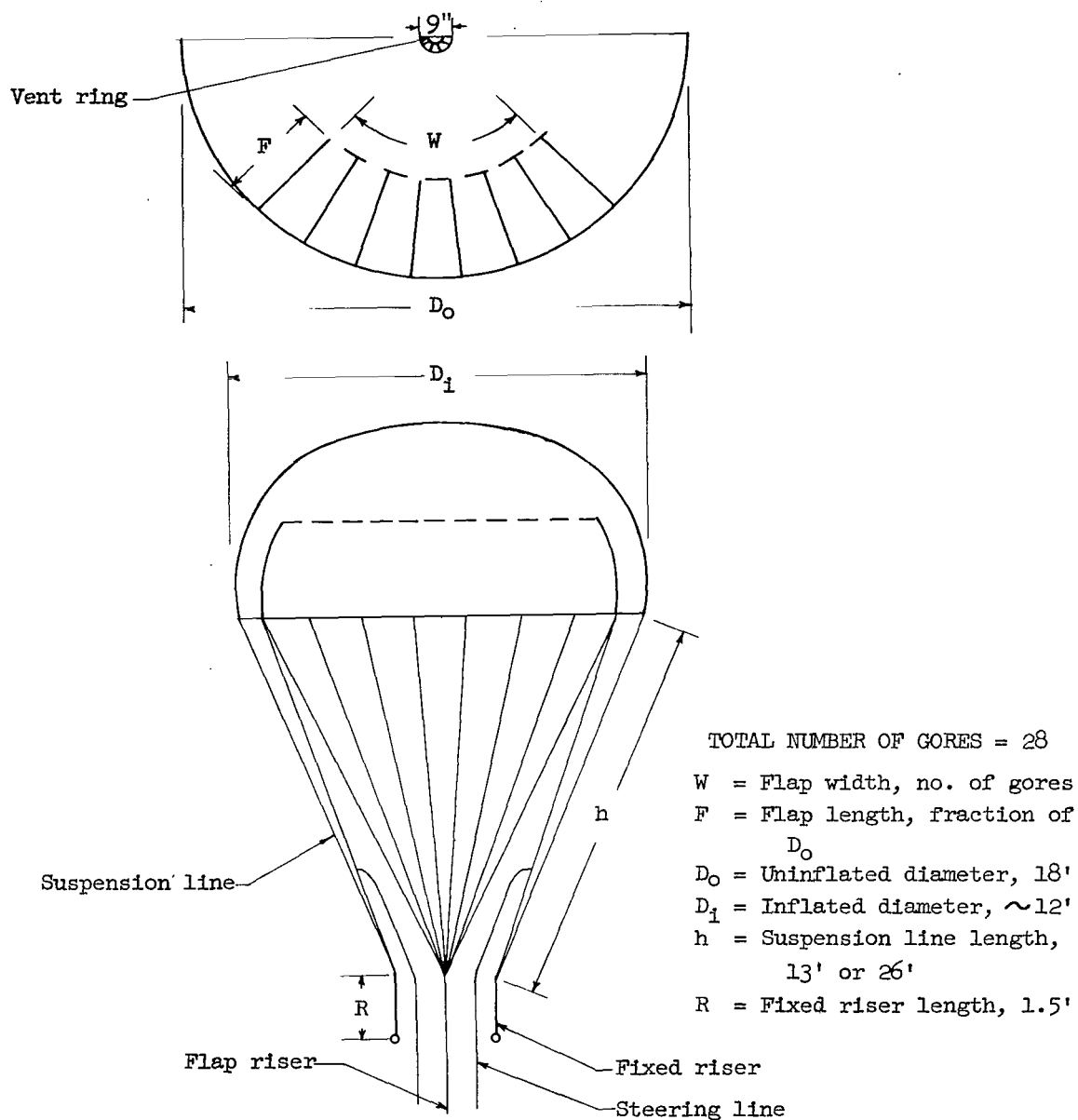
(a) Basic model dimensions.

Figure 1.- Description of the test model.
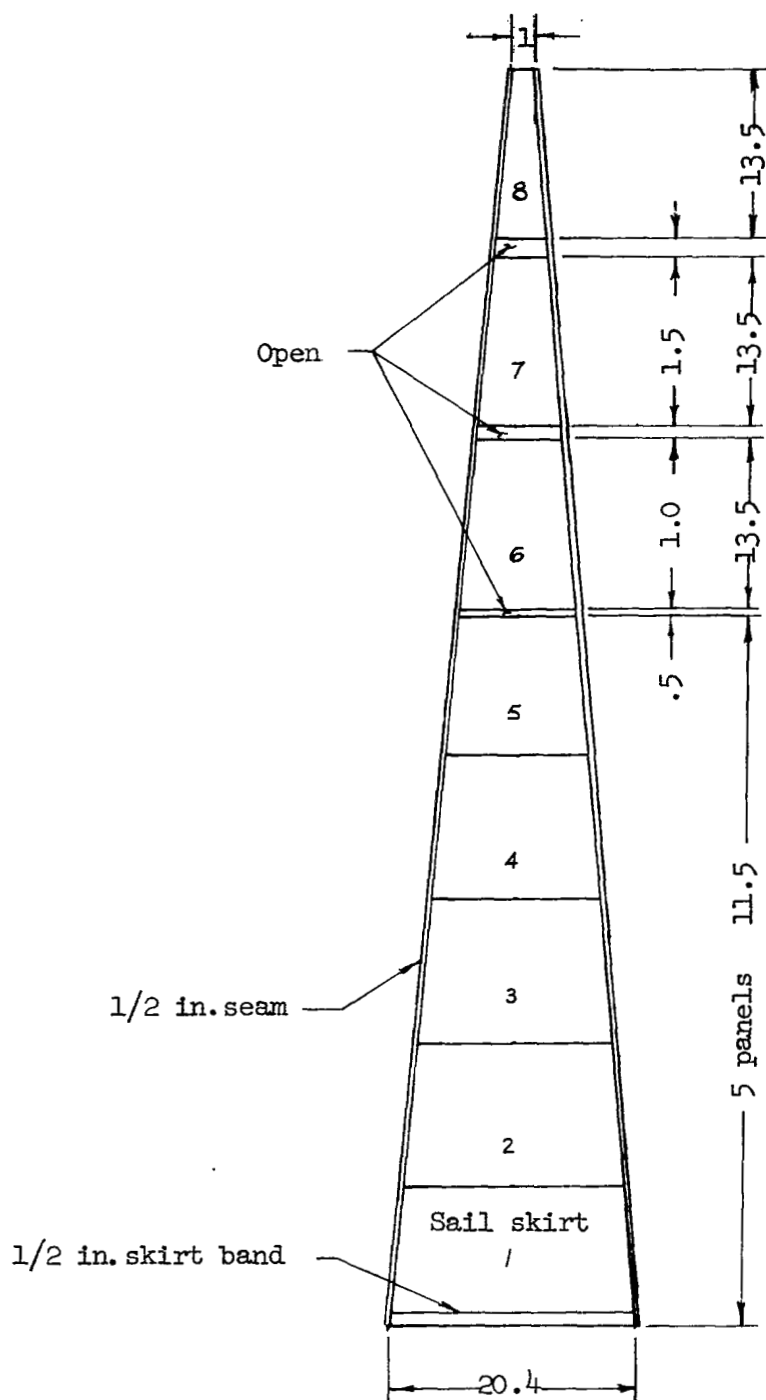
(b) Detail of parachute gore.

Figure 1.- Concluded.

A
6
3
3
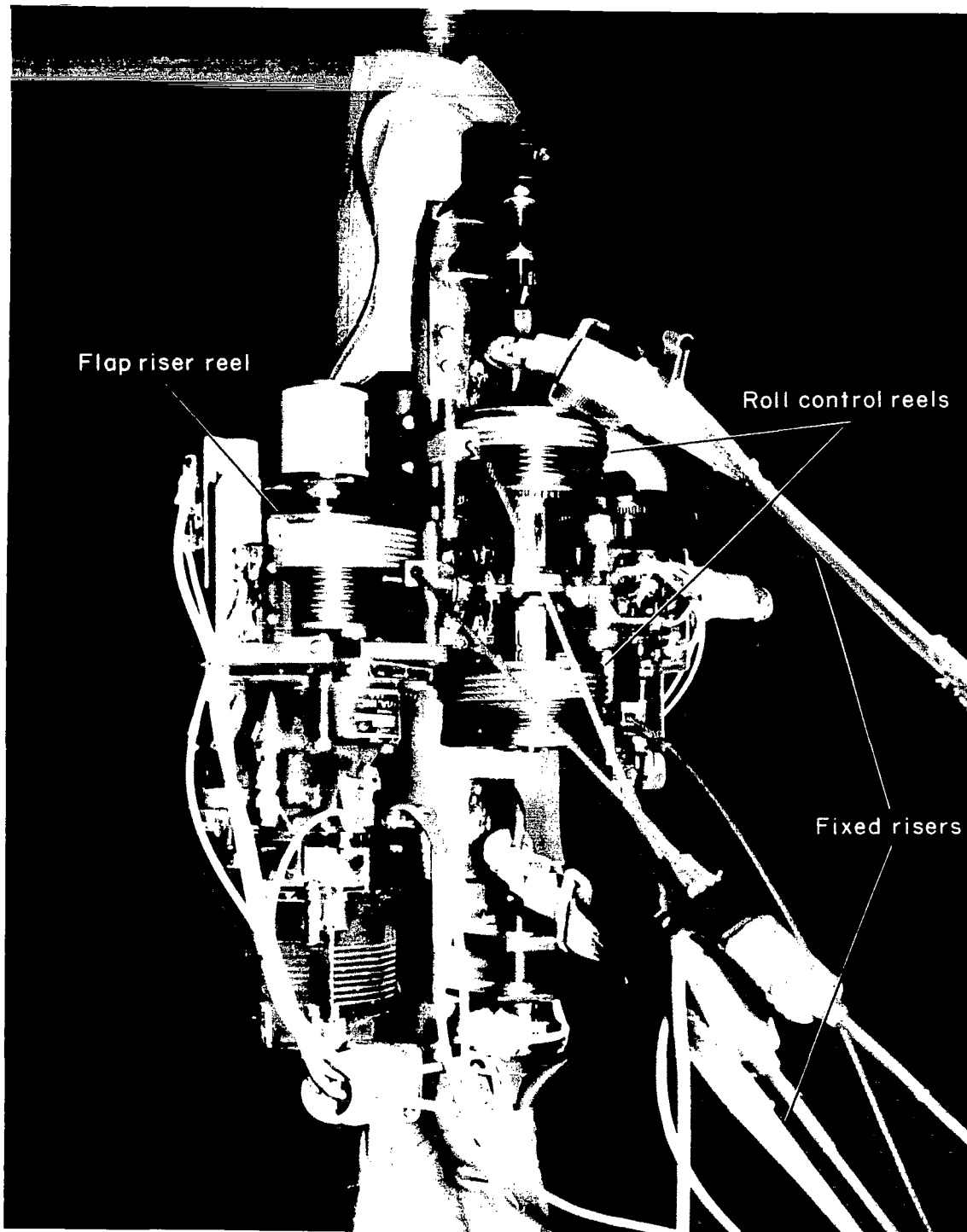
Figure 2.- The parachute support strut showing the control mechanism.

A-28302.1
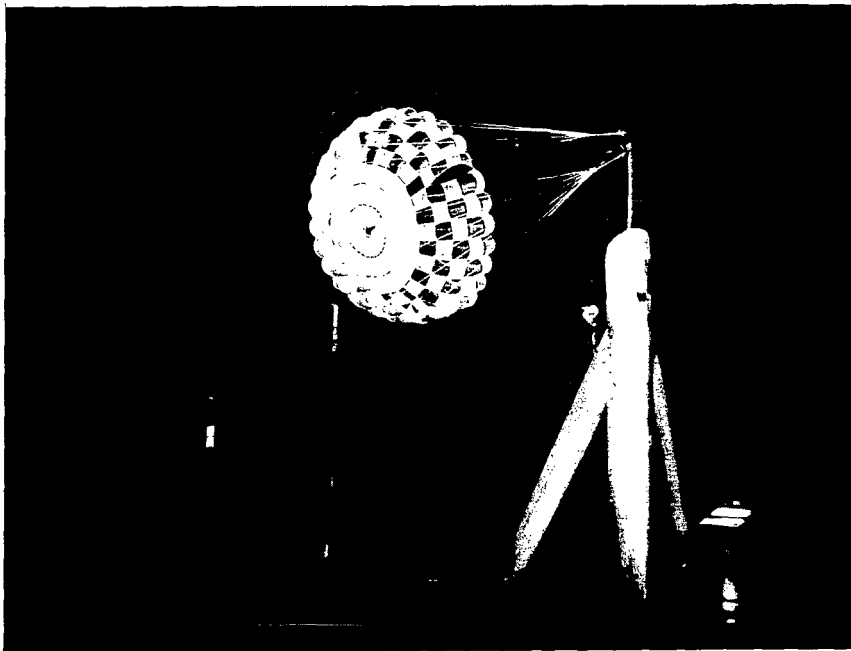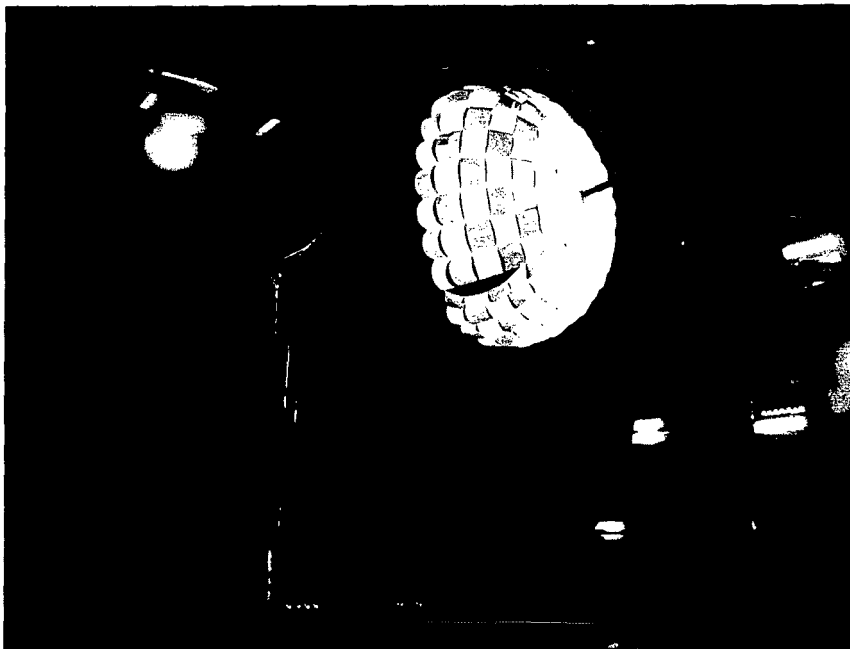
A-29215

A-29216

Figure 3.- A parachute model in the Ames 40- by 80-Foot Wind Tunnel.

Direction of travel

Sting

Two-component
balance

B

Six-component
balance

Direction of
travel

V

Support strut

$\alpha = \text{arc tan } (A/B)$

A
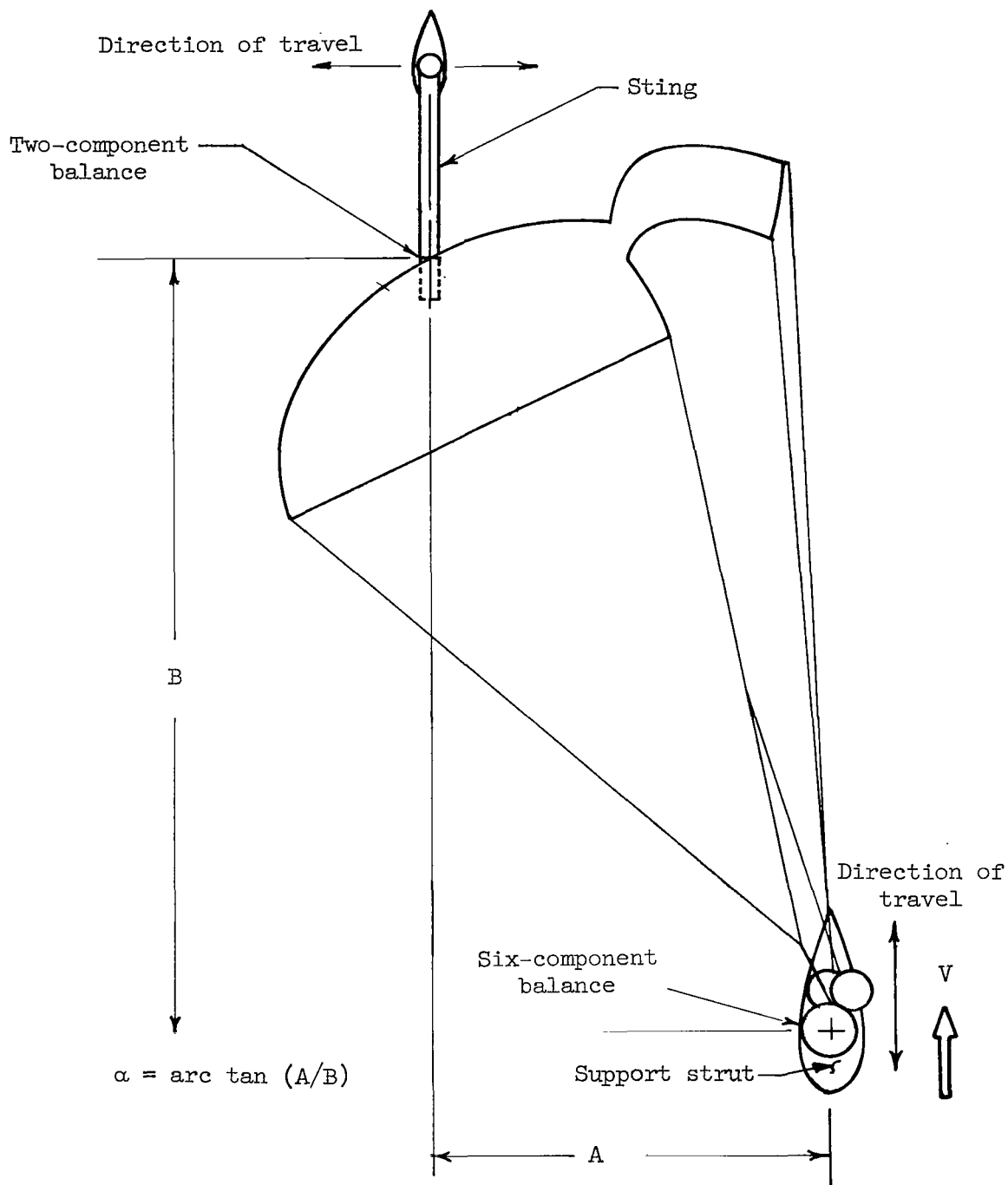
Figure 4.- Schematic diagram of the model in the wind tunnel showing
the method of determining the angle of attack.

14
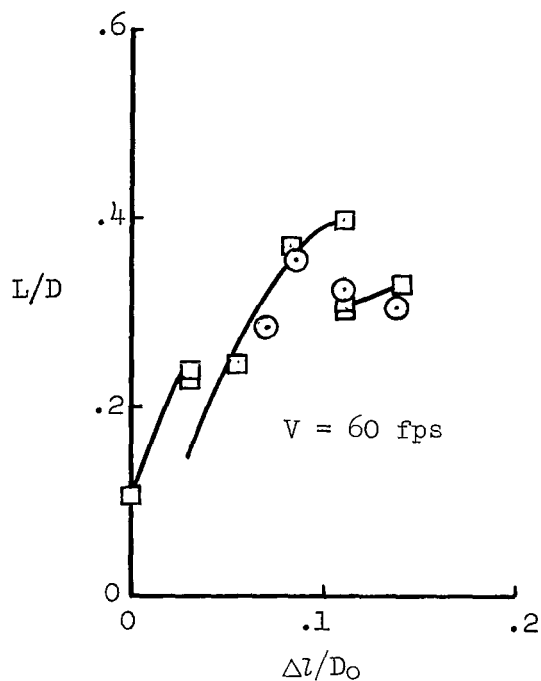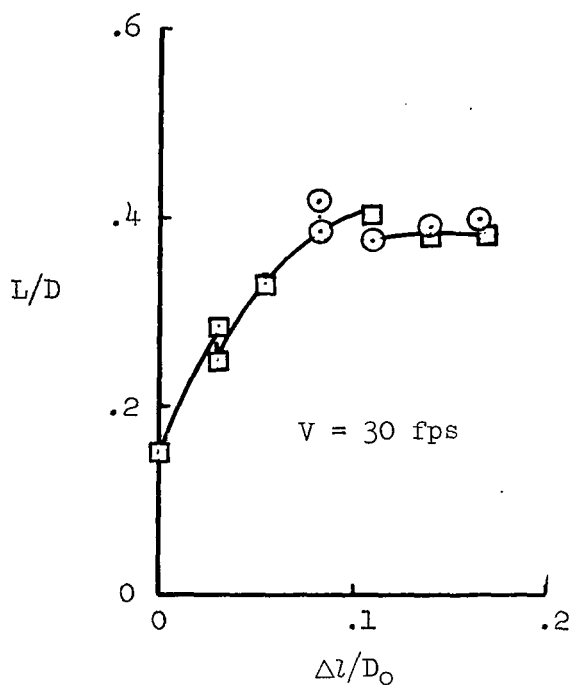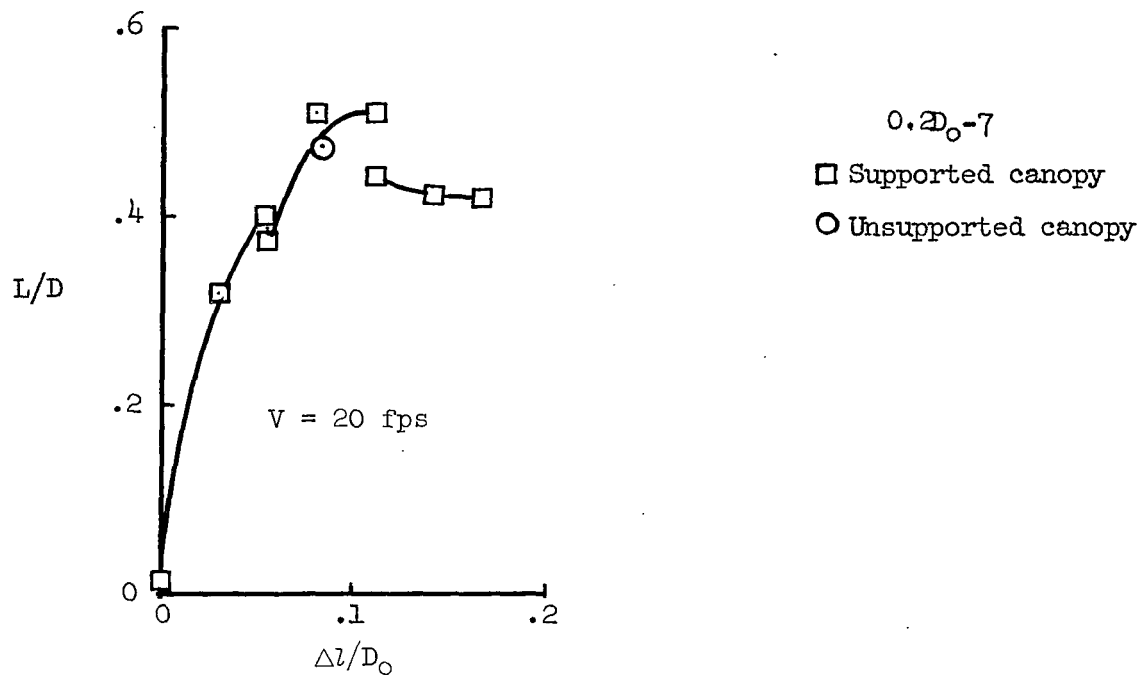
Figure 5.- The effect of the support sting on the lift-drag ratio
characteristics; $0.2D_O$-7 configuration, h = 13 feet.
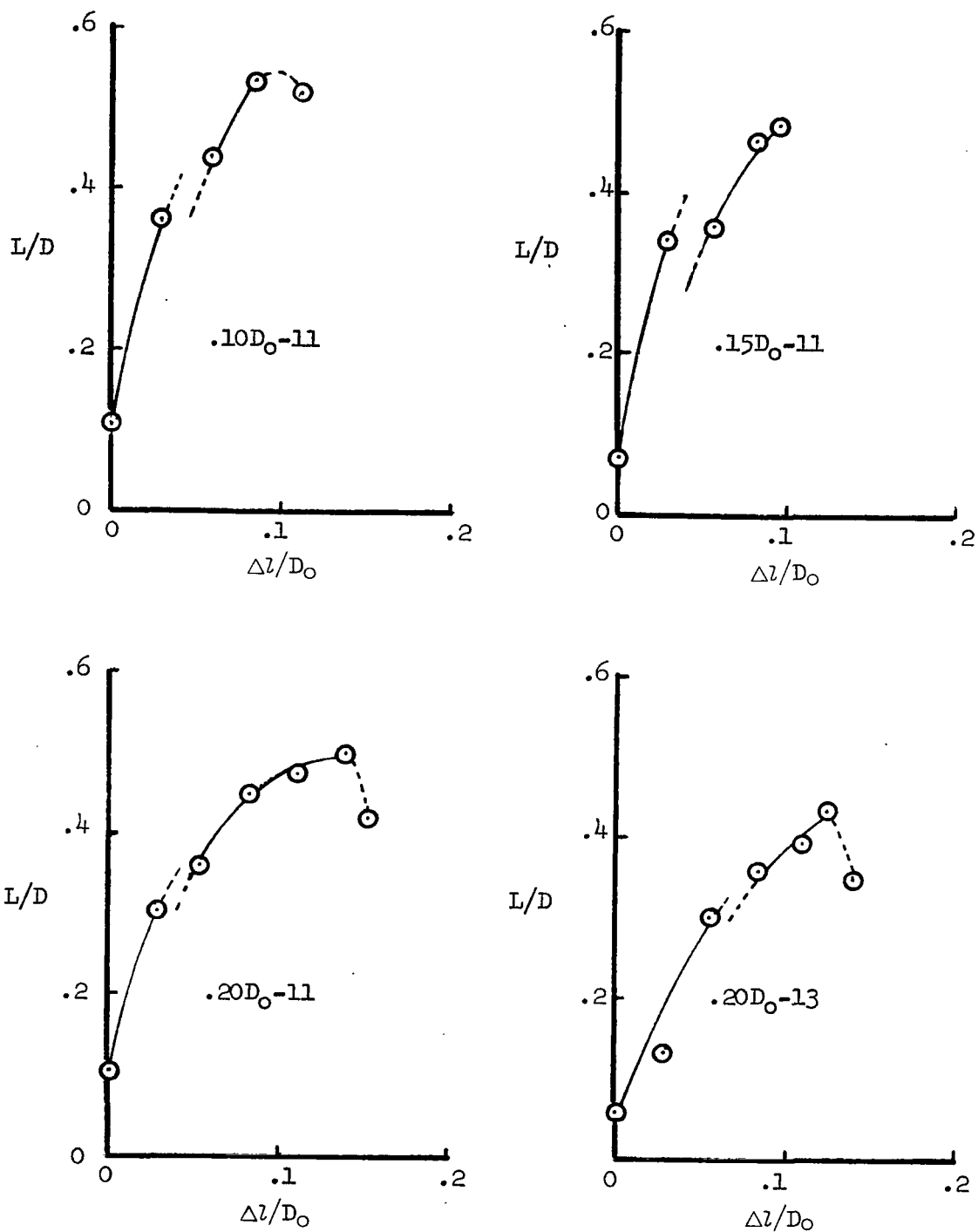
(a) V = 20 fps

Figure 6.- Lift-drag ratio as a function of flap extension for models
with 13-foot suspension lines at several free-stream velocities.
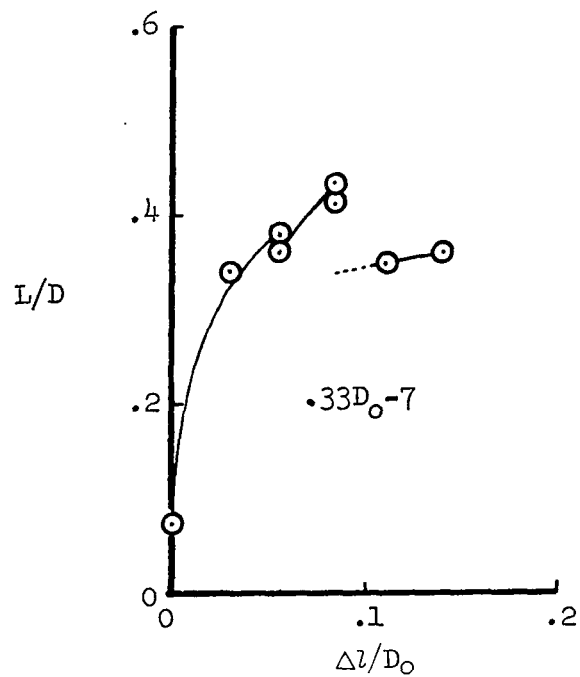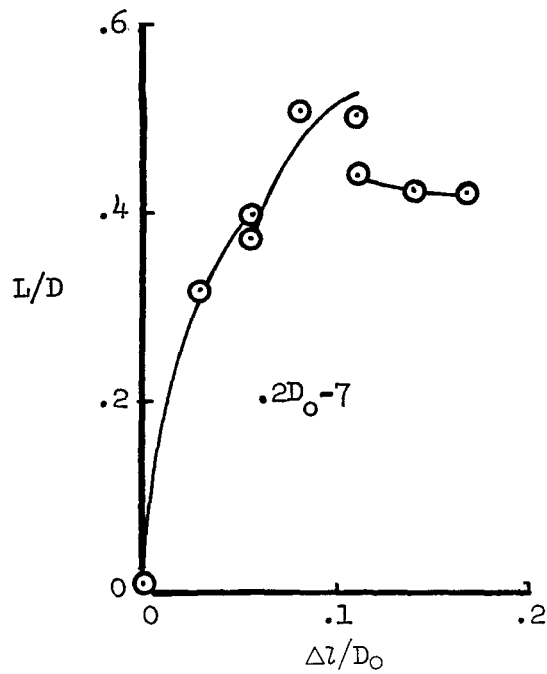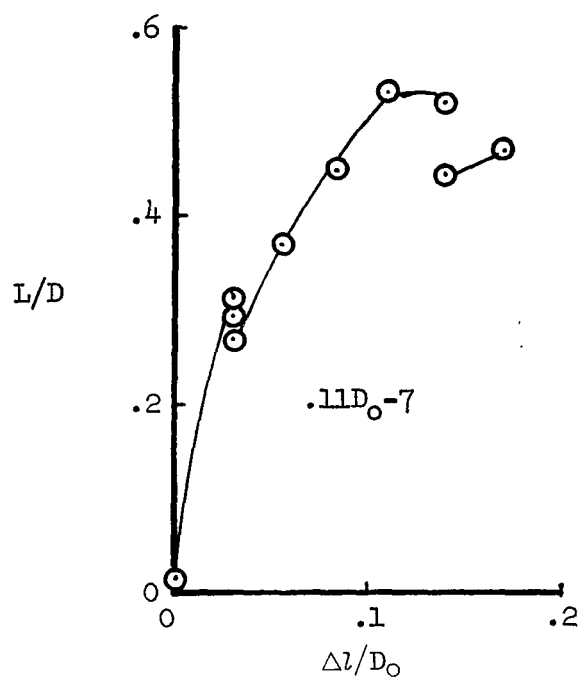
(a) V = 20 fps – Concluded.

Figure 6.- Continued.

A
6
3
3
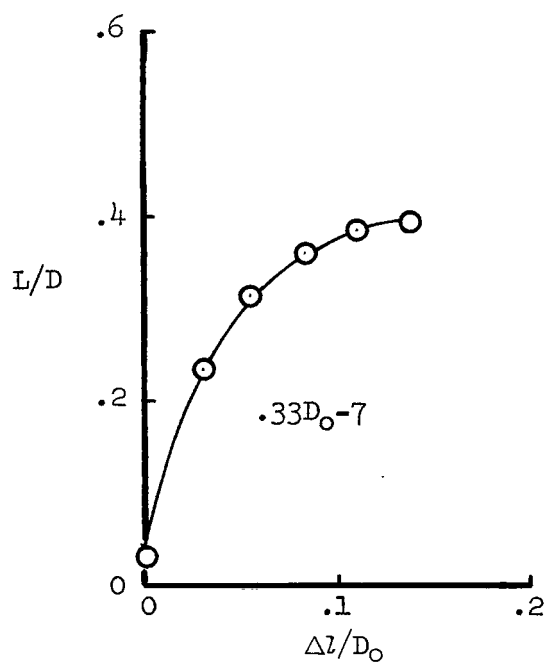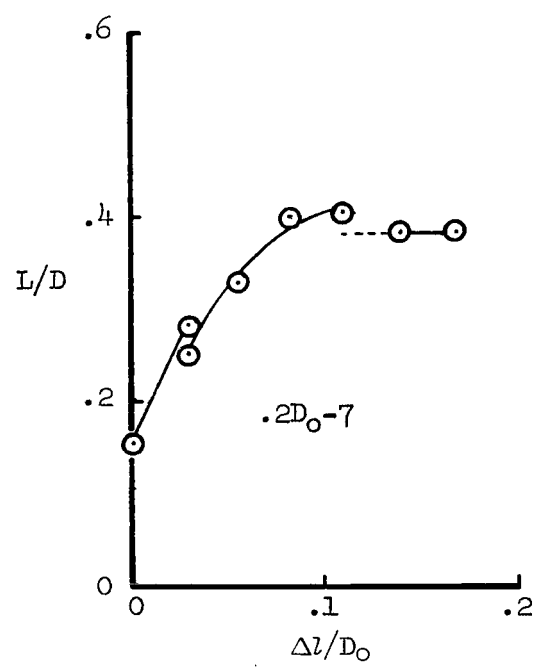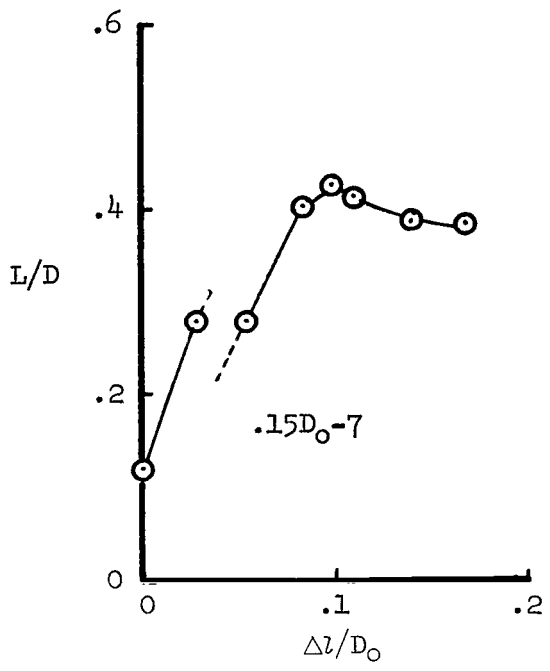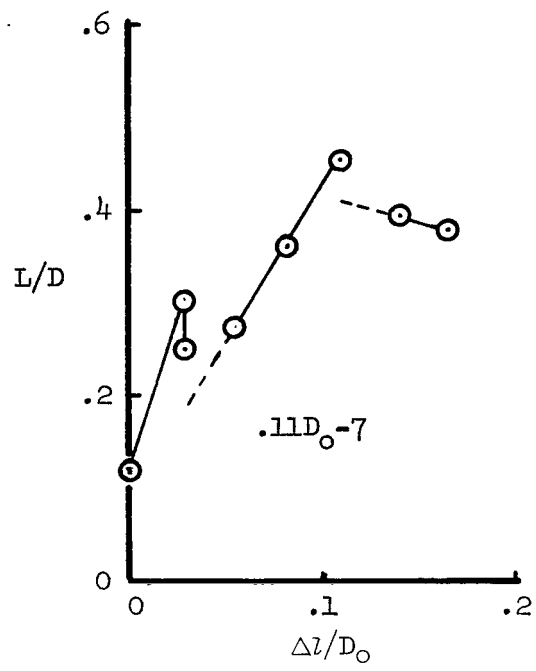
(b) V = 30 fps

Figure 6.- Continued.
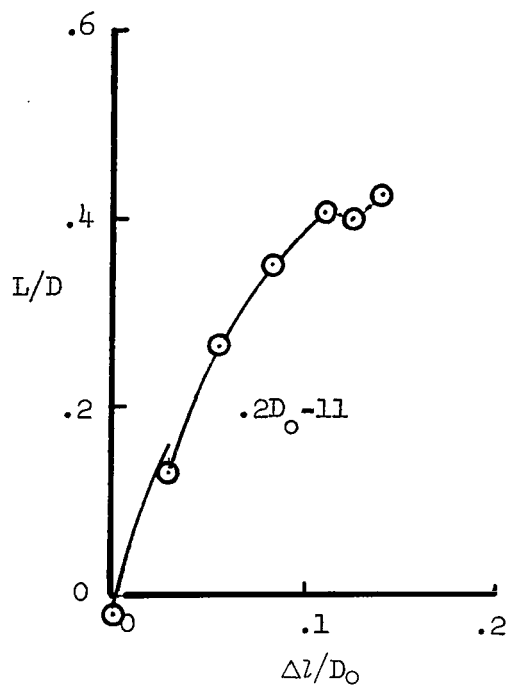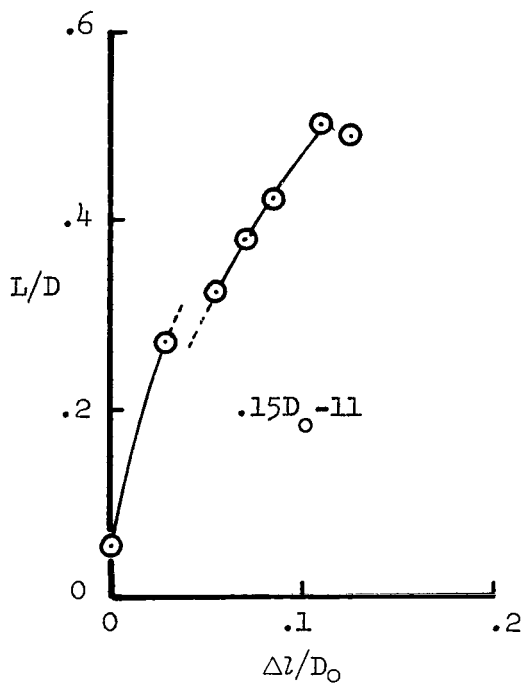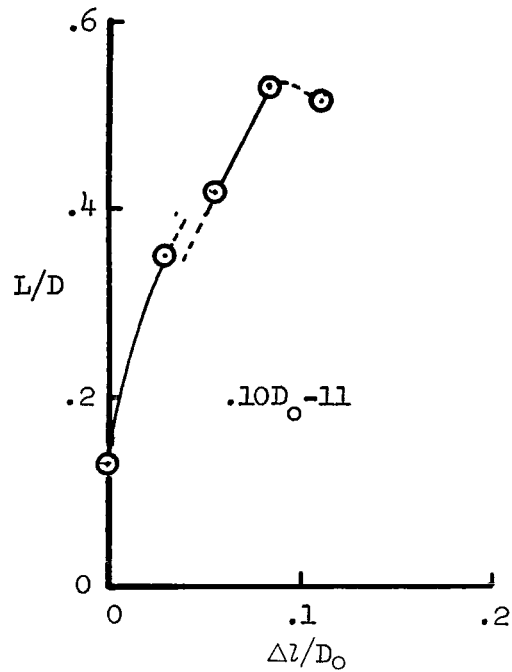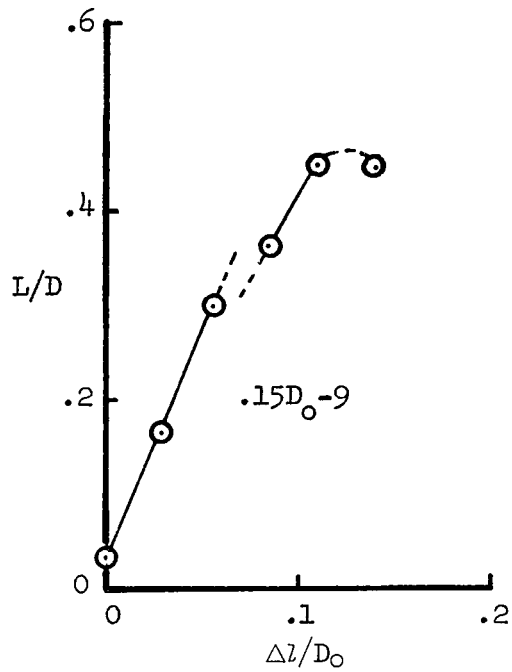
(b) V = 30 fps – Continued.

Figure 6.– Continued.

.6

L/D

.4

.2

0

.2D$_O$-13

0   .1   .2

$\Delta l/D_O$

.6

L/D

.4

.2

0

.15D$_O$-11

0   .1   .2

$\Delta l/D_O$

.6

L/D

.4

.2

0

.15D$_O$-13

0   .1   .2

$\Delta l/D_O$

.6

L/D

.4

.2

0

.2D$_O$-11

0   .1   .2

$\Delta l/D_O$
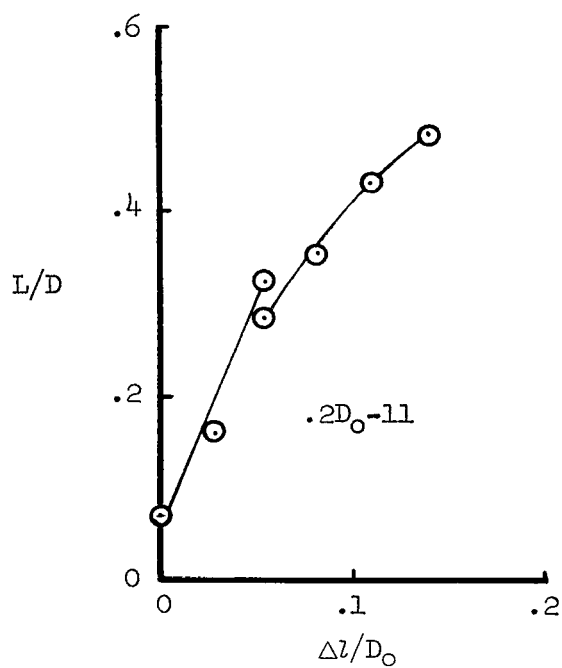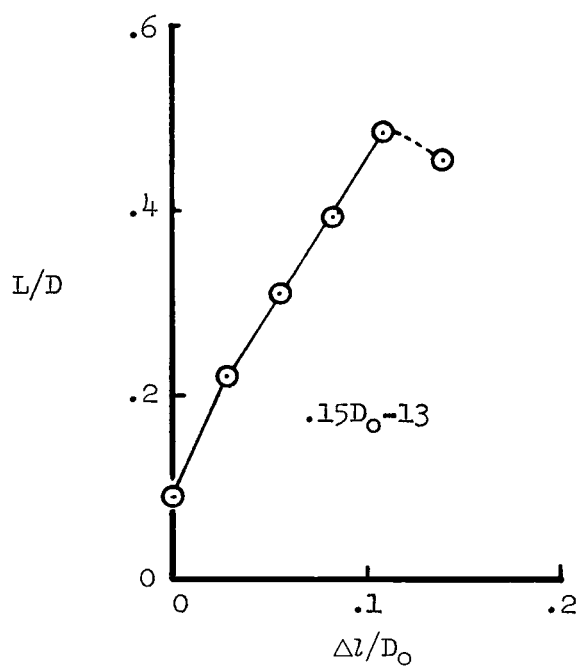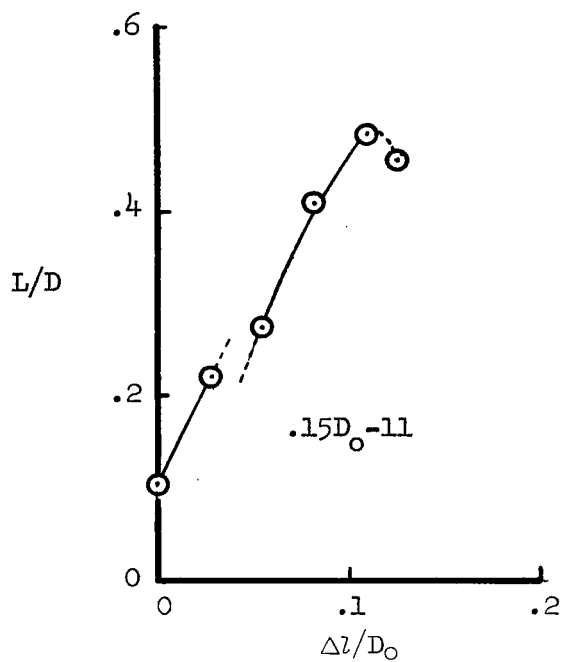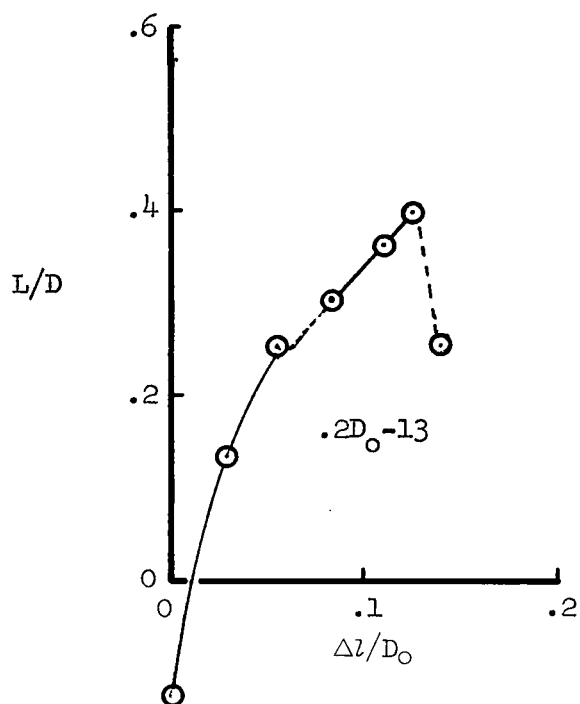
(b) V = 30 fps – Concluded.   (c) V = 40 fps

Figure 6.– Continued.
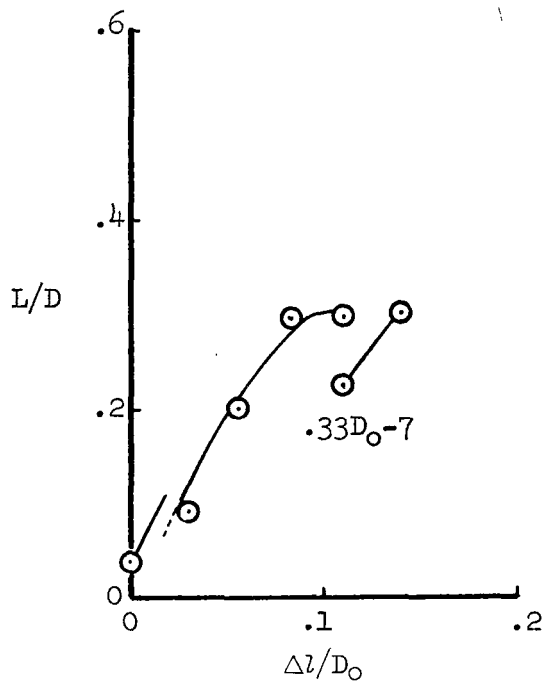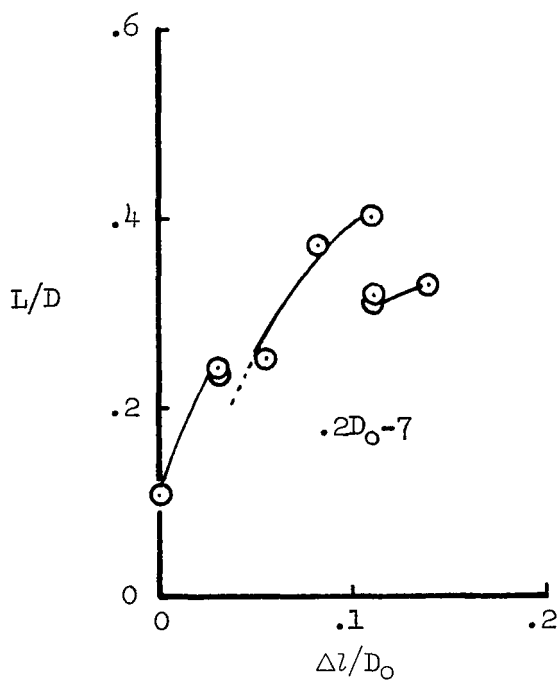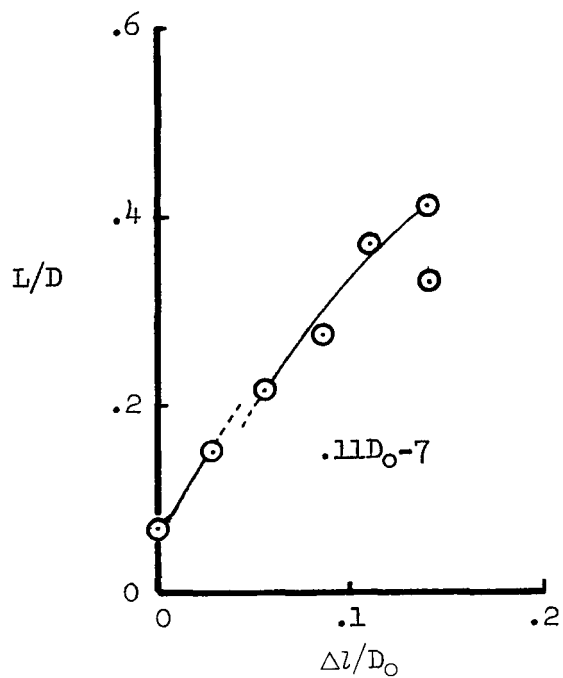
(d) V = 60 fps

Figure 6.- Concluded.

Side View   Front View

$\Delta l/D_O =$
.028

$\Delta l/D_O =$
.028
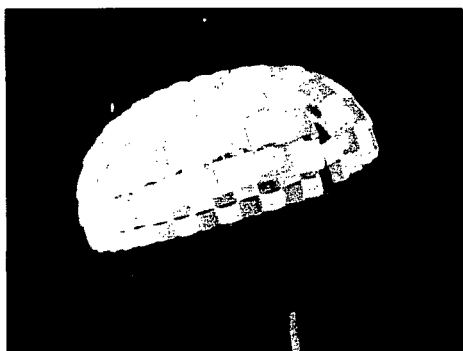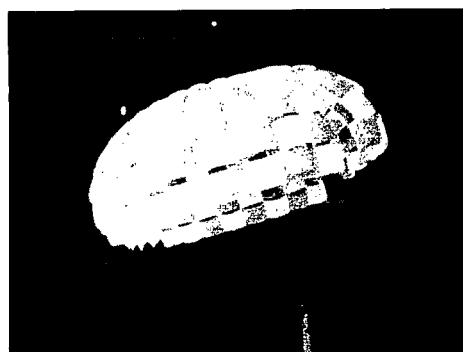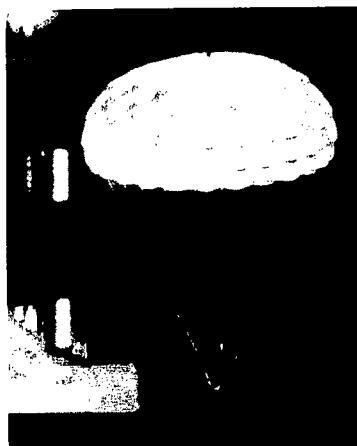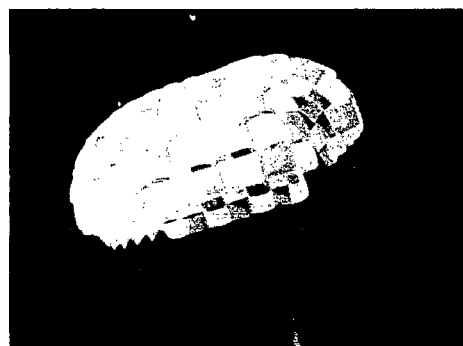
$\Delta l/D_O =$
.056

(a) First sail skirt.

Figure 7.- Progression with flap extension of the collapse of the
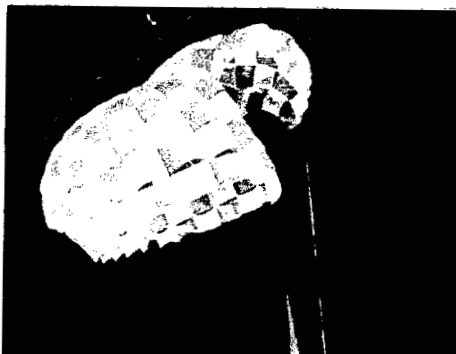leading-edge sails of the $0.2D_O$-7 configuration; V = 30 fps.

Side View   Front View
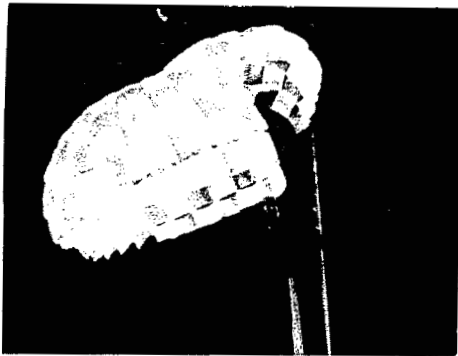
$\Delta l/D_O =$

.11
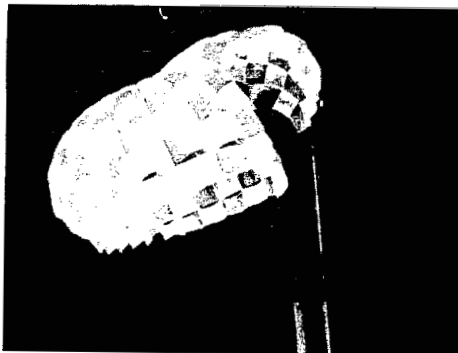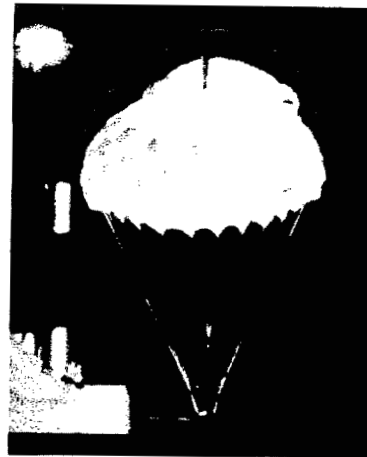
$\Delta l/D_O =$

.11

$\Delta l/D_O =$
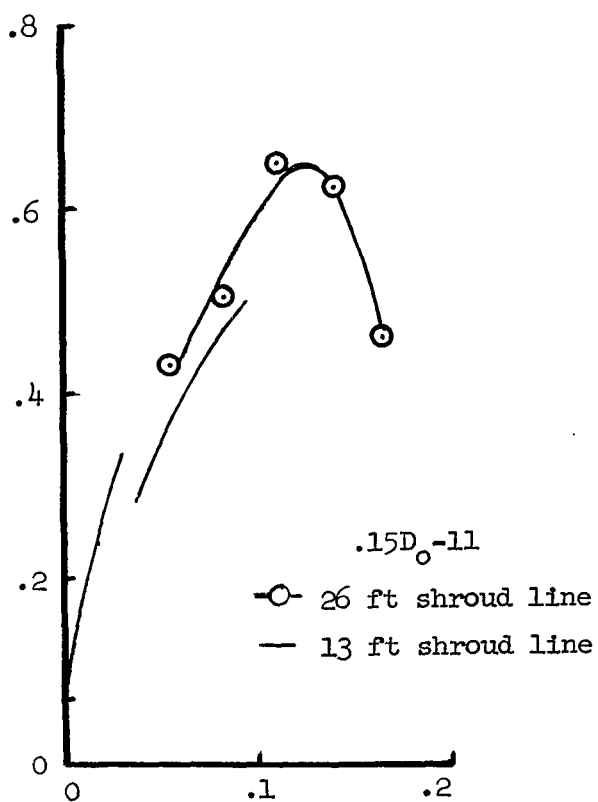
.139

(b) Second sail skirt.

Figure 7.- Concluded.

A
6
3
3

Figure 8.- The effect of increasing suspension line length from 13 feet to 26 feet on the L/D characteristics of the $0.15D_O$-11 configuration; V = 20 fps.
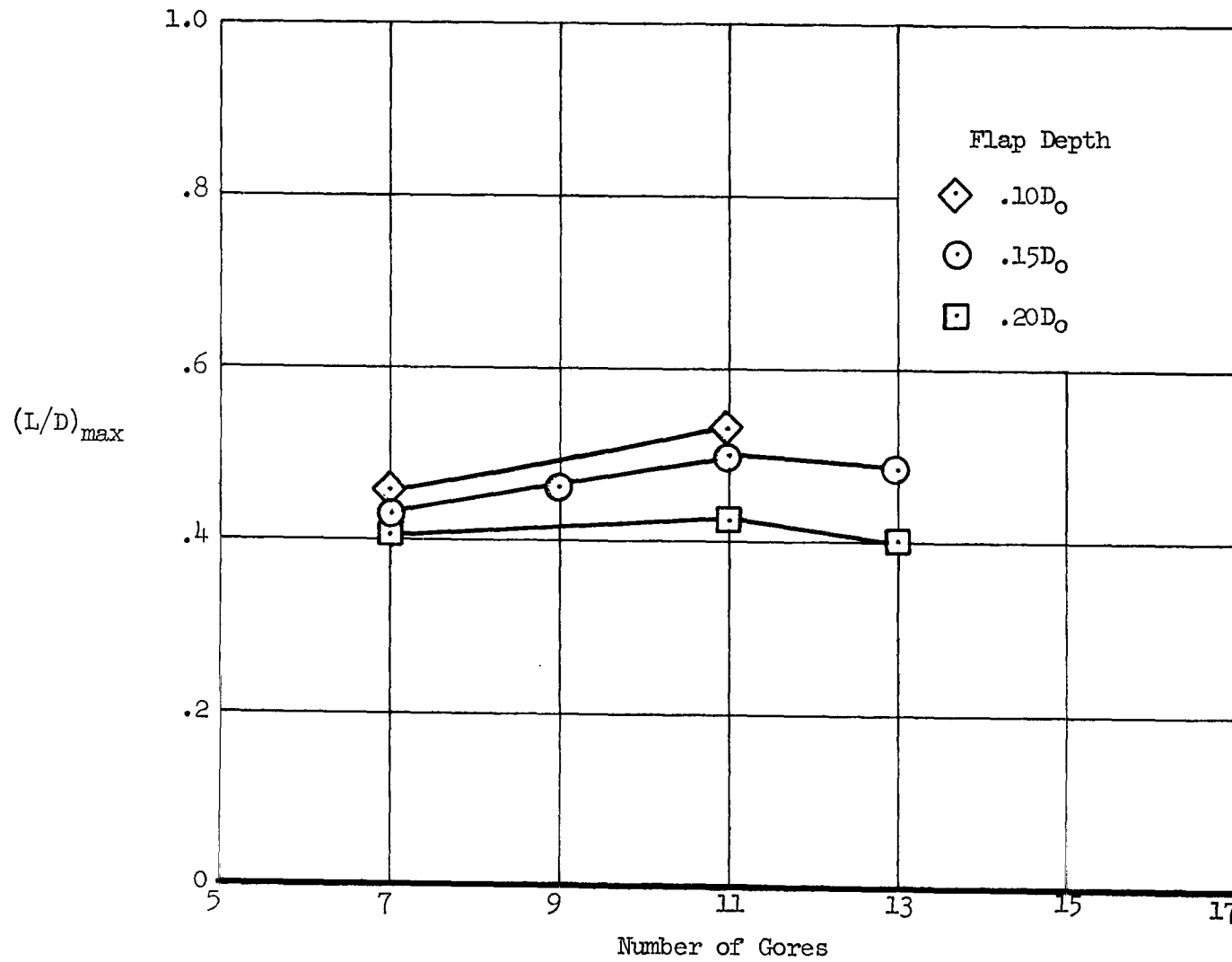
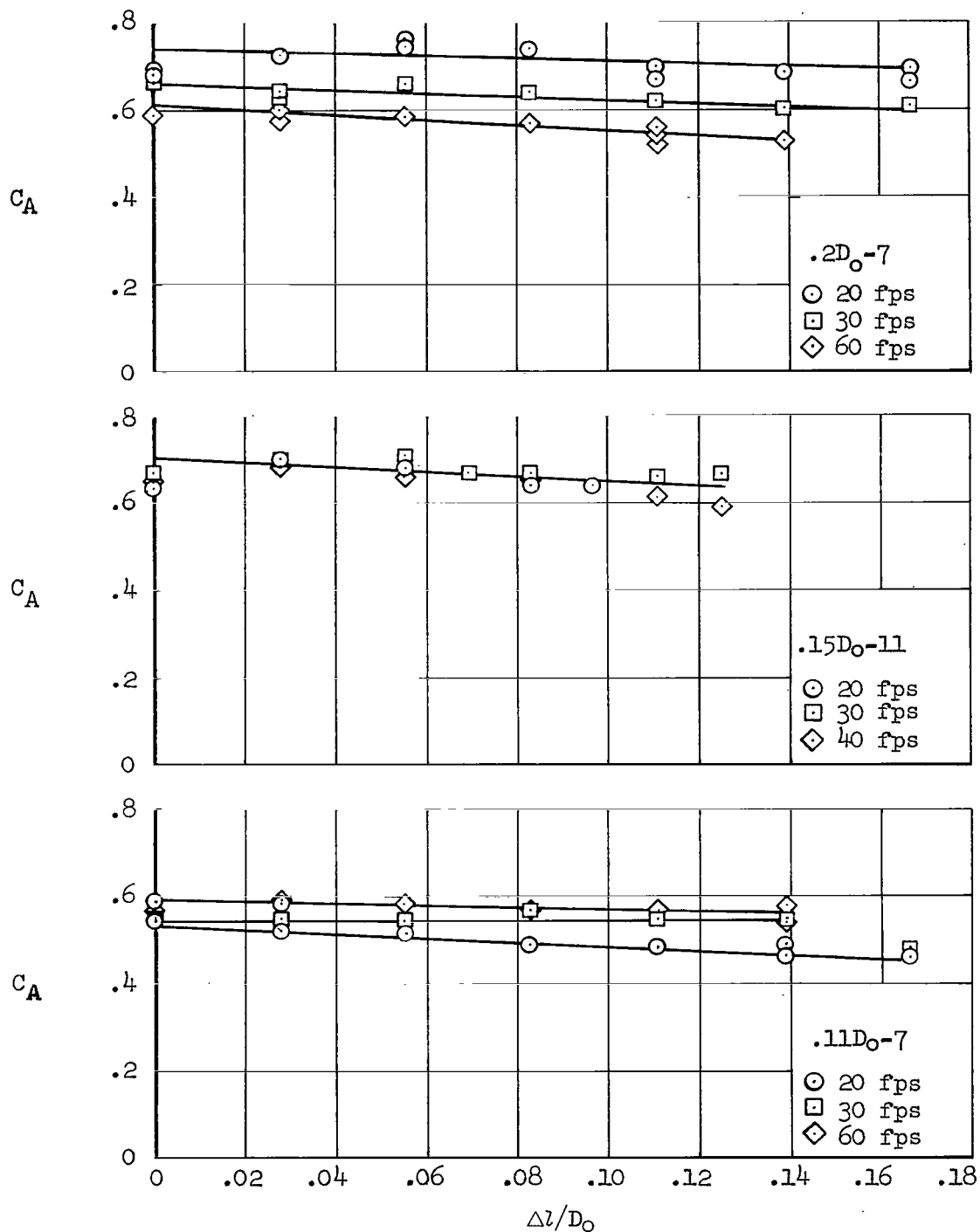Figure 9.- The effect of flap configuration on the maximum L/D; V = 30 fps.

Figure 10.- The effect of flap extension on the axial-force coefficient
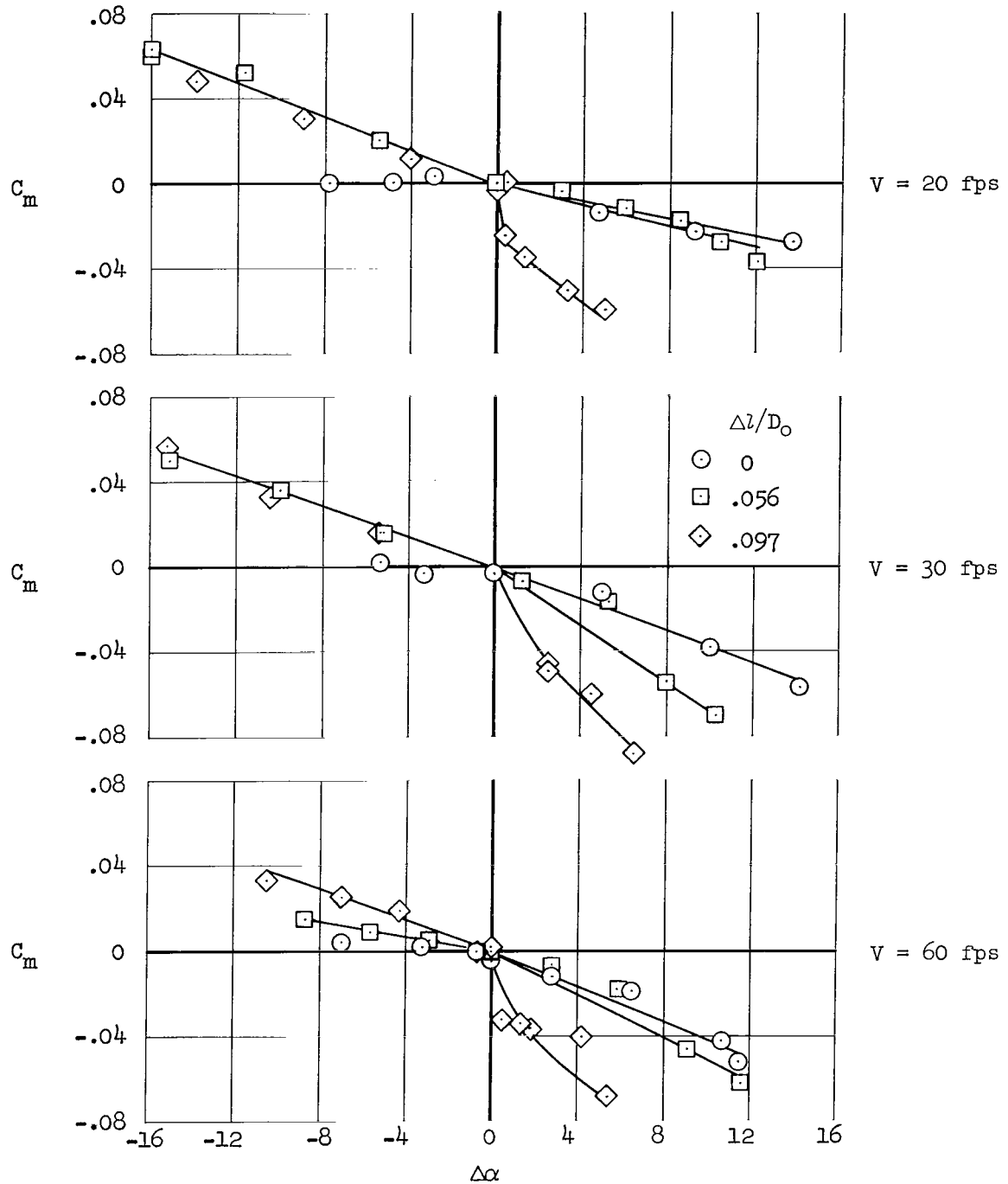for several flap configurations.

26

Figure 11.- Longitudinal stability characteristics of the $0.2D_O$-7 configuration; h = 13 feet.
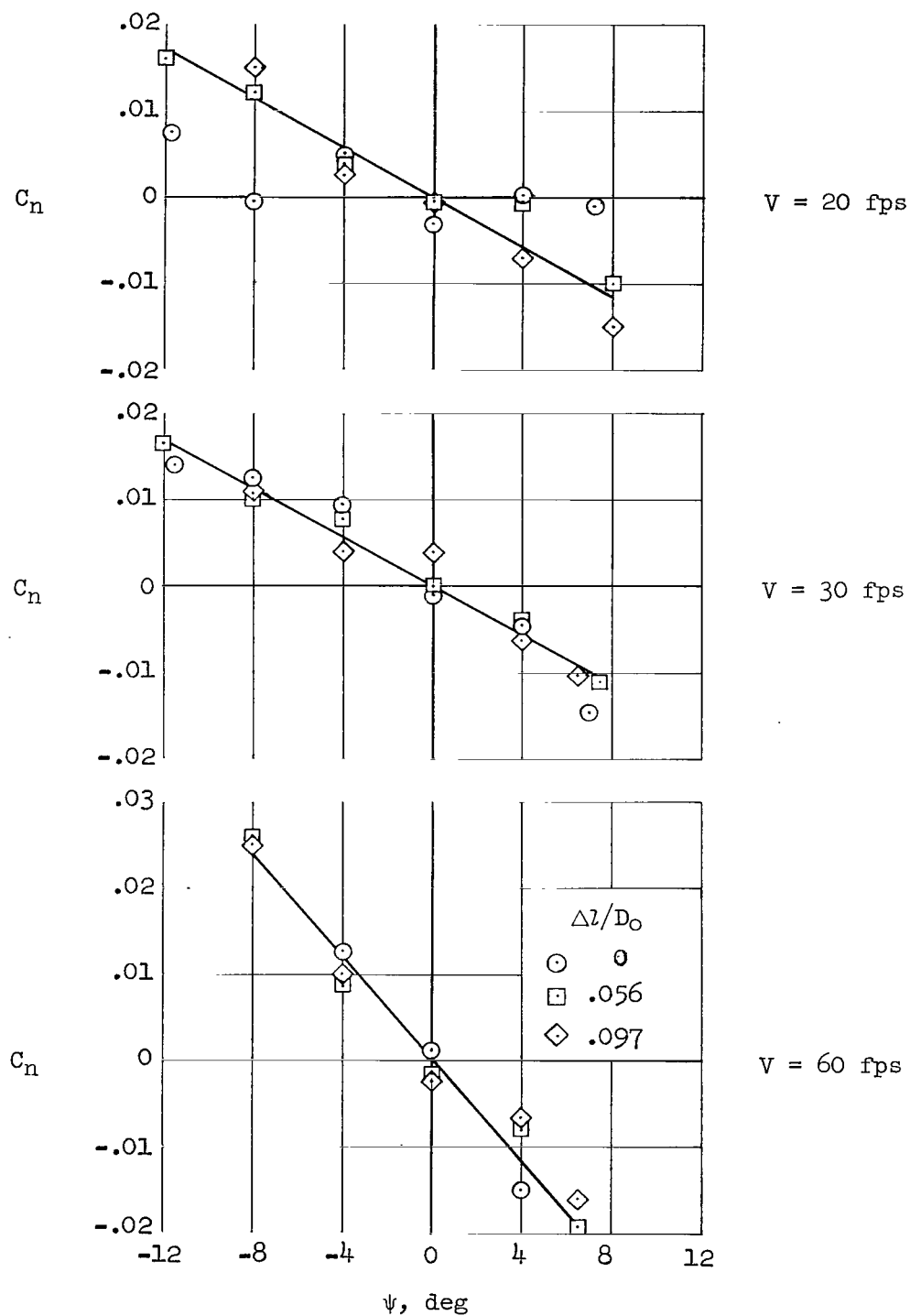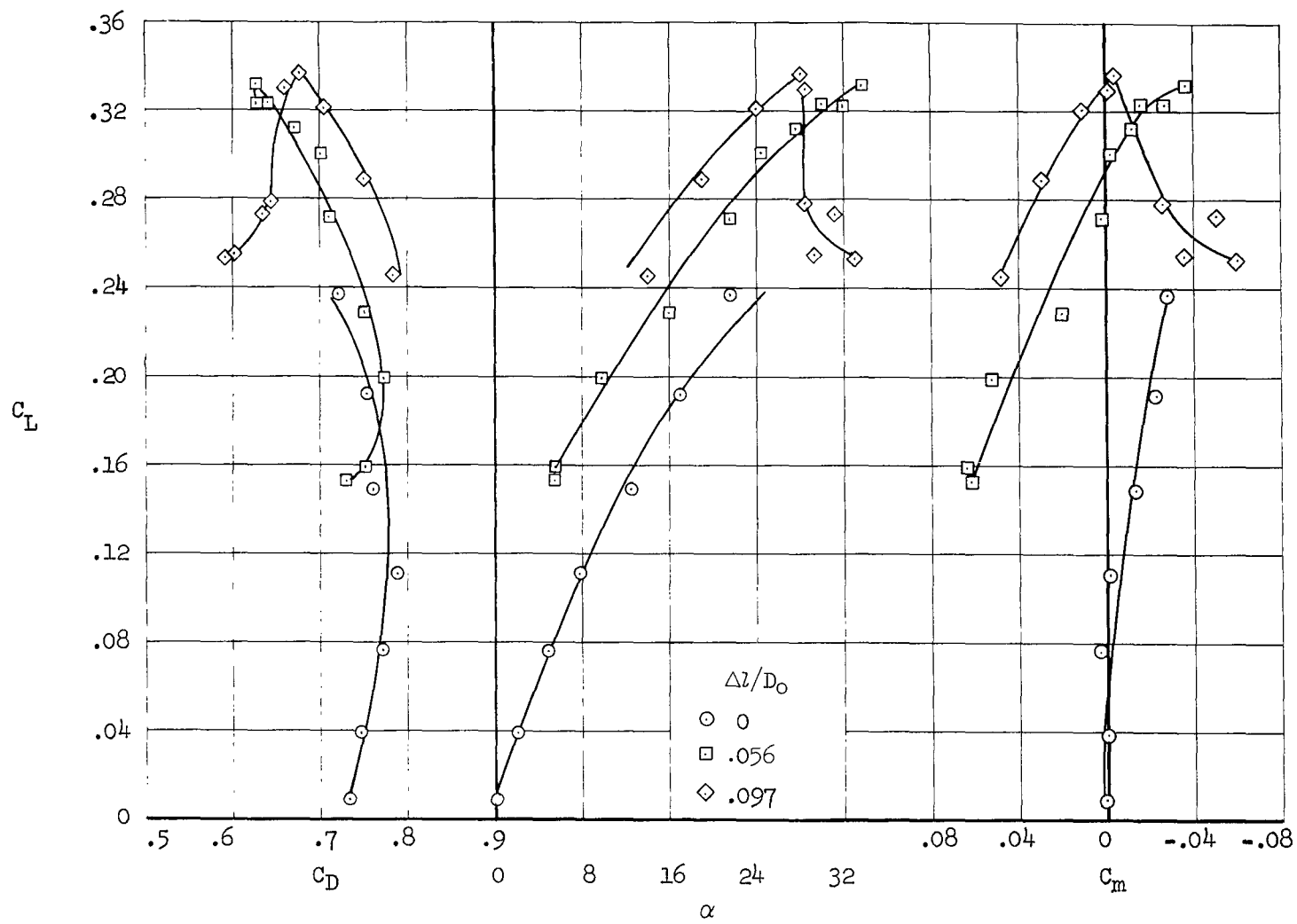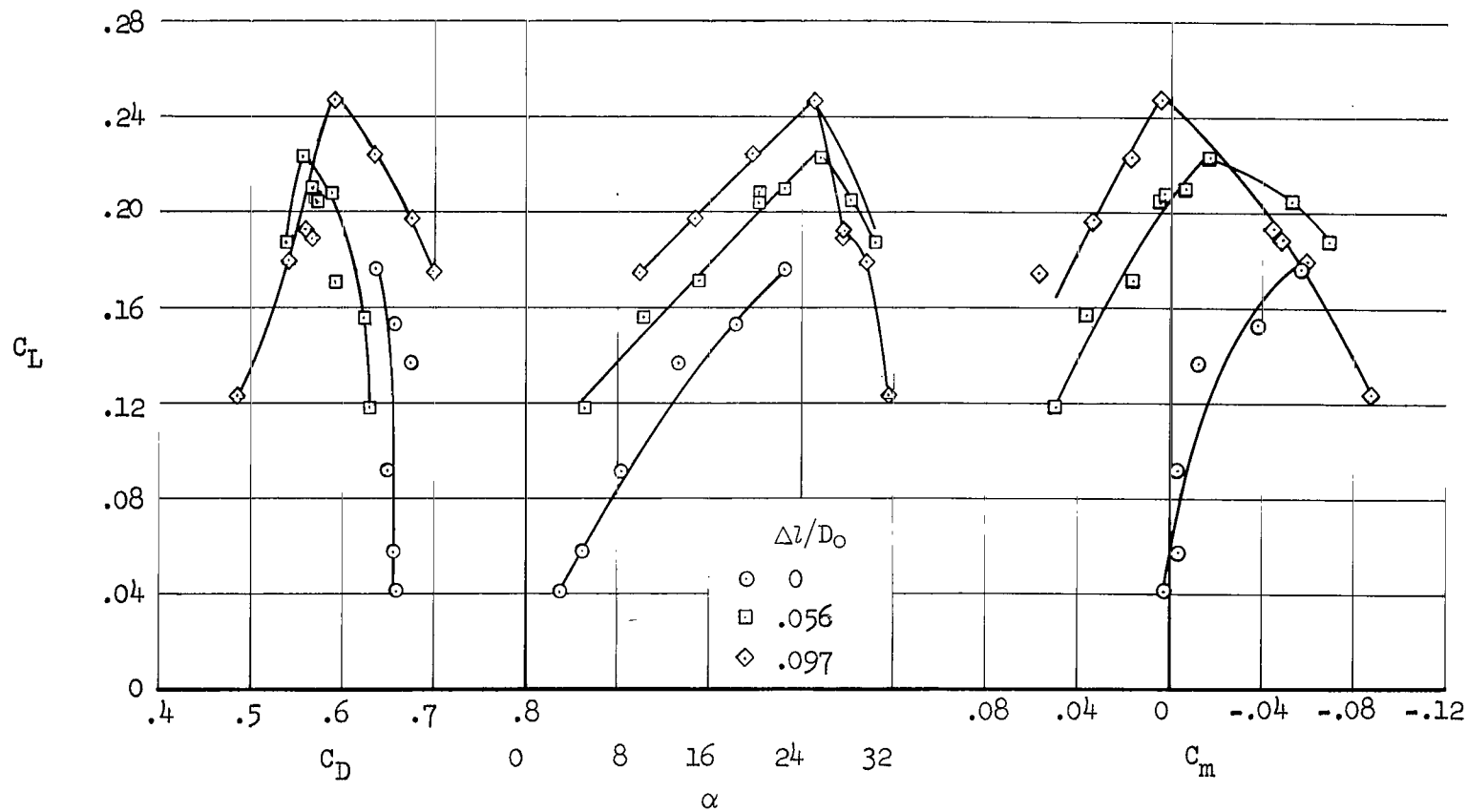
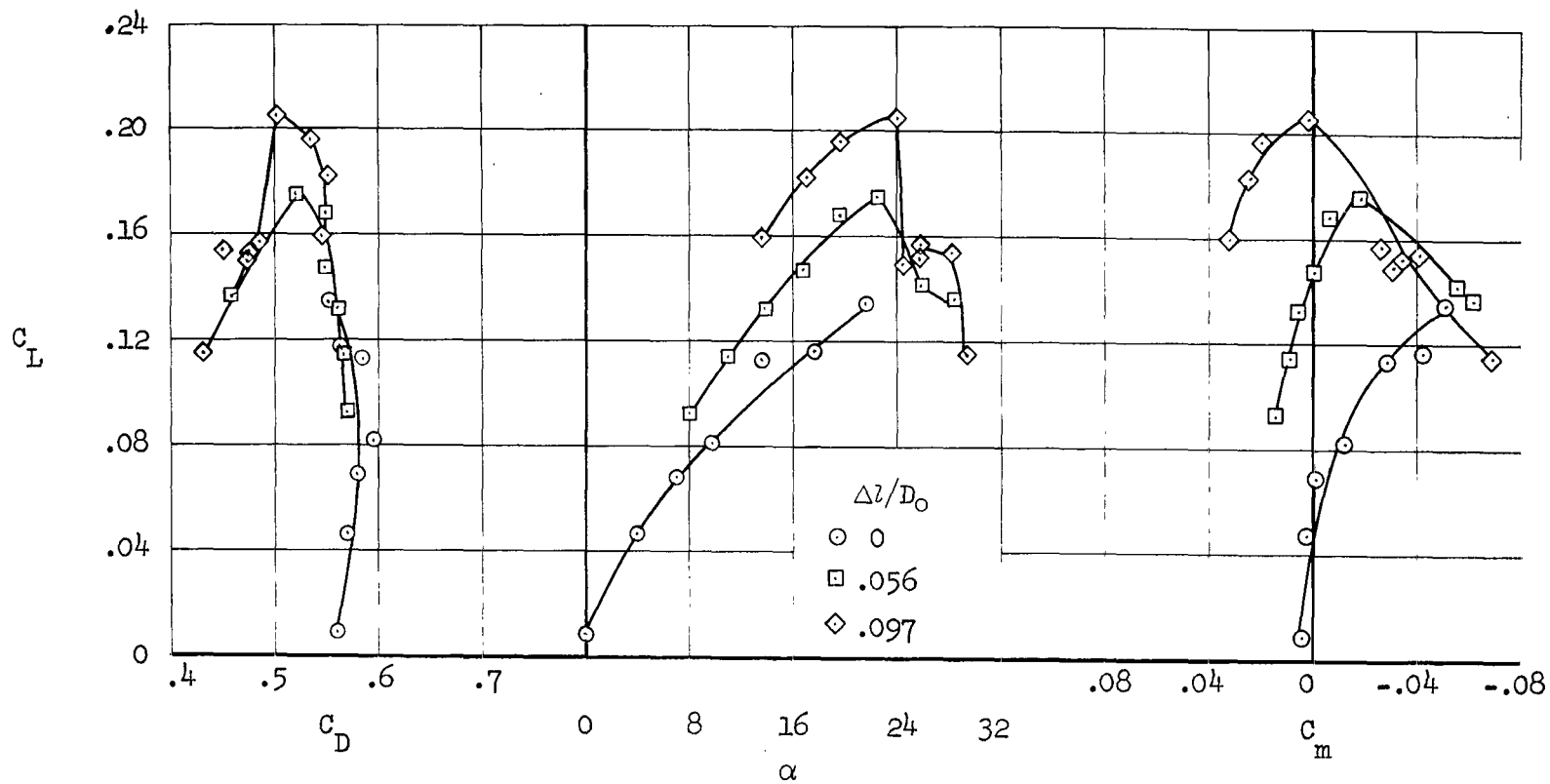Figure 12.- Lateral stability characteristics of the $0.2D_o$-7 configuration; h = 13 feet.

(a) V = 20 fps

Figure 13.- Aerodynamic characteristics of the 0.2D_O-7 configuration; h = 13 feet.

(b) V = 30 fps

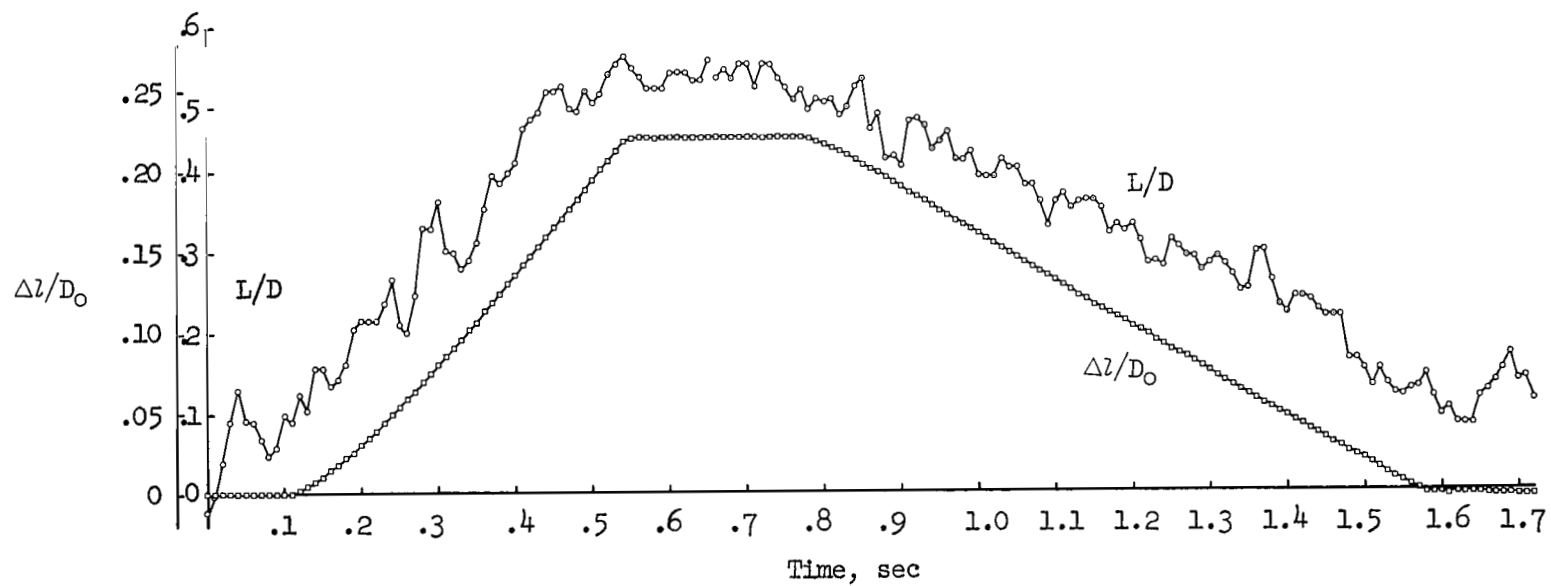Figure 13.- Continued.

(c) V = 60 fps

Figure 13.- Concluded.

Figure 14.- Time history of L/D and flap extension for the 0.2D$_O$-7 configuration; V = 30 fps, h = 13 feet.

NASA TN D-1334

A motion-picture film supplement is available on loan. Requests will be filled in the order received. You will be notified of the approximate date scheduled.

The film (16 mm, color, 10 min.) shows the Glidesail parachute at typical test conditions in the Ames 40- by 80-Foot Wind Tunnel. Tests are at a tunnel velocity of 30 feet per second. The parachute configuration had a flap $0.2D_0$ long and 7 gores wide.

Requests for the film should be addressed to the

    National Aeronautics and Space Administration
    Office of Scientific and Technical Information
    Technical Services Division (Code AFSS-A)
    Washington 25, D. C.

CUT
- -

Date_____

Please send, on loan, copy of film supplement to NASA
TN D-1334

_____
Name of organization

_____
Street number

_____
City and State

Attention Mr._____

        Title_____